Journal of Multidisciplinary Engineering Science and Technology (JMEST)
ISSN: 2458-9403
Vol. 5 Issue 11, November - 2018

The Effects Of Hydrogen Injection On Ultra Lean Combustion In Diesel Engines

Gerald J Micklow, Helge von Helldorff, Ehsan Tootoonchi
Dept. Mechanical and Aerospace Engineering
Florida Institute of Technology
Melbourne, FL 32901, USA
gmicklow@fit.edu

***Abstract* - In the presented study, the effects of the ingestion of a stoichiometric hydrogen-oxygen mixture into the inlet air at engine speeds of 1300 and 3300 rpm on a Yanmar 6LY2A-STP marine Turbo-Diesel engine at rates that can practically be produced by on-board hydrogen generation systems were investigated through numerical simulations using the KIVA 3V CFD software. Hydrogen ingestion showed increases in peak temperature and pressure, increased fuel evaporation and earlier onset of combustion, along with a more complete burn of the hydrocarbon fuel.**

With the exception of the 1300 rpm case with 1% H2-O2 mixture, which showed a net efficiency increase of 1.3%, net thermal efficiency decreased with hydrogen ingestion for all cases. Hydrogen ingestion through on-board hydrogen production was thus found unsuitable to increase net engine efficiency, unless the hydrogen can be produced through systems utilizing otherwise rejected energy, e.g. through recuperation of exhaust thermal energy.

Keywords—Combustion; Diesel; hydrogen; dual-fuel; CFD modelling; compression ignition

I. INTRODUCTION

Today, the world faces tremendous energy, economic and environmental challenges. Significant changes in the production and consumption of energy must take place to minimize adverse energy and environmental impacts. Currently, 93% of the energy consumed in the US comes from non-renewable fossil and nuclear fuel. Transportation accounts for 67% of the petroleum consumed and the transportation sector is 97% dependent on oil, accounting for a consumption of 572 million gallons of petroleum based fuel every day in the US in 2004 alone. Furthermore, with a steady increase in the number of vehicles and miles traveled, air quality problems in our cities continue to worsen. It is now recognized that one of the “clean” products of complete combustion, CO_2, is a strong contributor to the greenhouse effect, and may ultimately be the most dangerous by-product. Global fuel conservation and a reduction of our reliance on foreign oil supplies, as well as environmental concerns are compelling reasons to find cost-effective solutions to both reduce our consumption of energy and transition to renewable sources. This requirement for transition has led to the introduction of increasingly strict emissions standards, taxes on emissions and bans of high-emission vehicles in high-traffic areas around the world in order to incentivize efficiency in the transportation sector.

The internal combustion engine, being the near exclusive mode of power generation in the ground transportation sector, is thus of essential interest in the push to increase fuel efficiency and reduce pollutant emissions. In particular, the Diesel engine has become increasingly popular, as it offers improved fuel conversion efficiency, greater torque over a wider engine operating speed, and lower CO2 emissions compared to gasoline engines.

Marked increases engine efficiency and reduce pollutant emissions can be achieved by improving the combustion process and/or changing the type of fuel burned. To this end, dual fuel combustion schemes have received significant attention from the research community. These dual fuel engines utilize small quantities of various pilot fuels, often ingested with the intake air or port-injected, to improve the ignition, evaporation and combustion processes.

Poonia et al. showed experimentally that the addition of LPG to the intake air of Diesel engines can leverage in brake thermal efficiency increases on the order of 4-11% compared to standard Diesel operation and depending on engine load while significantly decreasing HC emissions [1].

Similarly, Quadri et al. achieved brake thermal efficiency improvements of 2-6% by substituting between 10 and 20% by mass of Diesel with hydrogen enrichment of the intake air through the improvements in the combustion process [2]. The secondary fuel had only a small contribution to the total engine heat release but improved engine efficiency by increasing flame speed and ensuring a more complete combustion process for the base fuel.

Since the increased NOx emissions of compression ignition engines in comparison to spark ignited gasoline engines are intimately tied to the fuel injection process and the in-cylinder fuel distribution and the ensuing combustion process, a secondary fuel may be injected in small quantities to improve the combustion process. In this study, hydrogen was used as the secondary fuel.

A small amount of hydrogen added to the intake air-fuel charge permits the engine to operate with leaner air-to-fuel mixture than otherwise possible. [3]

For lean fuel mixtures, peak combustion temperature decreases substantially effectively mitigating NOx production. With hydrogen injection, it is expected that lean or ultra-lean engine operation can be obtained without a substantial performance decrease. Under idle conditions, reduced loads and moderate acceleration, hydrogen addition in combination with lean burn engine conditions can produce acceptable operation with a marked reduction in pollutant emission formation and fuel consumption [4], [5], [6].

The concept of hydrogen enrichment for a petroleum based fuel or renewable biofuel for use in an internal combustion engine configuration has a greater interest than pure hydrogen powered engines because it involves fewer modifications to the engines and their fueling system.

This concept assumes that hydrogen will be generated on-board the vehicle from electrolysis of water where the required electricity is supplied by the vehicles charging system. While the laws of thermodynamics would intuitively suggest a decrease in efficiency due to energy conversion losses in such a system, it is believed that the introduction of hydrogen as a secondary fuel changes the ignition and combustion process such that the increase in combustion efficiency results in a net increase in engine efficiency.

The exact mechanism by which the increase in the combustion processes is achieved is still not very well understood and literature sources are often very contradictive in their conclusions. Thus, much of the research on hydrogen-enhanced Diesel combustion has been of experimental nature, partially due to the complexity and computational cost involved in incorporating complete chemical mechanisms in CFD models. However, experimental results have proven promising and have overall produced promising data, showing efficiency increases of up to 30%.

Most commonly, hydrogen injection is associated with decreases in ignition delay and the achievement of conditions closer to homogenous combustion than with only hydrocarbon fuels. An investigation on cylinder pressure variations in hydrogen-Diesel dual fuel engines, with hydrogen mass fraction of up to 3.5 percent at 1600 rpm showed that in all investigated cases peak pressure was shifted to later points in the engine cycle with increasing amounts of hydrogen injected into the cylinder. This is attributed to an increase in combustion delay occurs due to the higher auto-ignition temperature of hydrogen as compared to Diesel. [7].

Ref. [8] have conducted an extensive experimental study on utilizing hydrogen gas in direct injection Diesel engine under dual fuel mode. It was found that increased hydrogen flow rates produced greater power and efficiency, especially at lower engine loads, while the effects diminished at full load. However, this was limited by the onset of knock and combustion instability at high hydrogen flow rates of 9.5 Lpm. Further, peak pressures were slightly increased, which was attributed to higher heat release rates. It was found that hydrogen reduces the ignition delay by 1-2° crank angle, causing earlier onset of combustion, which along with the higher heat release rates increases cyclic efficiency [8].

Contradictory to these findings are the experimental results produced by [9]. The experimental study utilizing a fully instrumented 2L test engine with hydrogen enrichment of the inlet air between 0 and 8% by volume showed are reduction in thermal efficiency in all low engine speed, low-medium load cases, contradicting the findings by Saravanan et al.(2009). Further, a reduction in carbon emissions was shown with increasing hydrogen flow rates, while simultaneously a very significant increase NOx emissions by up to 30% due to increased combustion temperatures was measured, leading the author to suggest a hydrogen enrichment limit of 6% by volume for the investigated case. These findings correspond very well to the results presented in this computational study.

Ref. [10] on the other hand investigated much higher hydrogen ingestion rates, resulting in 50, 90 and 97% Diesel fuel replacement in terms of energy input into the cylinder. It was found that these extremely high hydrogen concentrations had detrimental effects on the engine performance and efficiency, due to the higher auto-ignition temperature of hydrogen resulting in ignition retardation and failure to completely ignite the hydrogen and Diesel mixture.

Utilizing a 71 species kinetic mechanism, with multiple NOx formation pathways including thermal NOx, Fenimore prompt NOx and N_2O intermediate mechanism, the research by [11] suggests that the increase in temperatures alone cannot account for the increases in NO_2 production experienced with increasing hydrogen ingestion. Instead, the increase in HO_2 from the ingested hydrogen facilitates the conversion of NO to NO_2. These results could not be reproduced in this study due to the much simpler 13 species Extended Zeldovich Mechanism being used, which combines NO and NO_2 species as a single NOx species.

Though it does not include any original research, the literature study presented by [12] does point out the important fact that the sharp increases in NOx and the positive effects on engine efficiency can only be obtained through proper tuning and adjustment of the engine timings and mixtures as compared to a pure Diesel combustion case due to the higher flame speed of the hydrogen gas. Like most studies, this study does not perform this additional engine tuning for comparability reasons and the exponential additional effort required in optimizing the engine for each hydrogen ingestion percentage.

Deb provides an experimental study of hydrogen-Diesel dual fuel engine operations. It was found that the engine in dual fuel mode required spark or glow plug assistance to initiate combustion of the hydrogen pilot fuel, as the auto-ignition temperature of hydrogen

is higher than that of Diesel. It was found that efficiency was increased in hydrogen-Diesel dual-fuel mode for all investigated cases. Further, the highest hydrogen injection case caused the highest efficiency gain of 18% over the standard Diesel mode, thus causing the highest reduction in BSFC by 15.25% [13].

The combustion kinetic models are of crucial importance to accurately model these multi-fuel combustion events.

An investigated the combustion efficiency and emissions for a hydrogen-Diesel dual fuel combustion system using chemical equilibrium analysis and minimizing Gibb's free energy in an iterative scheme for C15H27 showed that hydrogen addition resulted in slight increases in combustion temperature across all equivalence ratios, along with increases in all emissions species other than CO2, as the Diesel fuel was reduced [14].

Experimental analysis of the combustion process of a hydrogen-air mixture in a rapid compression combustor under CI engine conditions placed the hydrogen air mixtures in the detonation regime, resulting in very high heat release rates and combustion efficiencies [15].

This paper investigates the effects of the ingestion of a stoichiometric hydrogen-oxygen mixture into the inlet air at different engine speeds of a Yanmar 6LY2A-STP marine Turbo-Diesel engine at rates that can practically be produced by on-board hydrogen generation systems. While the heating value of the ingested hydrogen mixture is taken into account, a complete economic analysis of the system is outside the scope of this investigation and hydrogen production is assumed to not include any losses.

II. COMPUTATIONAL MODEL

The engine geometry modeled in the presented study was a Yanmar 6LY2A-STP marine Turbo-Diesel engine with a bore of 100 mm and a stroke of 110 mm. The piston bowl is off-centered from the z-axis, making the piston geometry non-symmetrical. The compression ratio of 15.2 ±0.5 as by the service manual was confirmed and determined to be 15.39 for the model presented here.

The computational study was performed using the KIVA 3V computational fluid dynamics code developed by Los Alamos National Laboratory. A 360° 3D mesh comprised of three uniform, structured blocks was analyzed for one cylinder and one engine cycle, starting at -180° (Bottom Dead Center (BDC) at beginning of compression stroke) to +180° (BDC at end of expansion stroke). The mesh was ensured to have smooth transitions between blocks and mesh study was performed, achieving a mesh-independent solution for meshes of more than 218394 cells.

The fuel injection process was modelled dynamically within KIVA at each time step and the number of fuel parcels was calculated based on the 5-hole injector nozzle geometry, featuring a total nozzle are of 0.54474 mm^2, the fuel injection pressure of 28.4 MPa, the injection timing, and the in-cylinder pressure distribution at the given time step.

TABLE I. ENGINE PARAMETERS

Compression Ratio	15.39
Bore	100 mm
Stroke	110 mm
# Mesh Cells	218394
Fuel Injector Type	5-hole
Total Injector Area	0.54474 mm^2
Fuel Injection Pressure	28.4 MPa

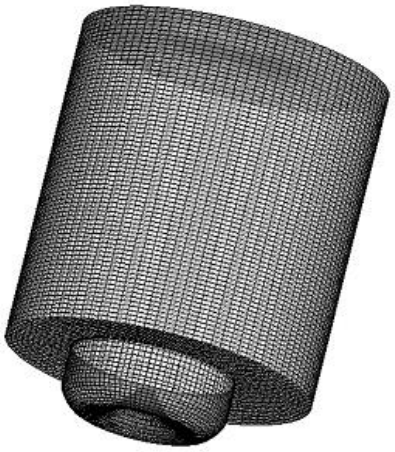

Fig. 1. 6LY2A-STP 360 degree Mesh at BDC

The stock injection timing provided by the service manual was -15° degrees to TDC at 1300 rpm with a linear injection timing advancement for higher engine speeds. The injection timings at increased engine speeds were determined by matching the modelled fuel flow rates with the linear injection timing advancement and brake specific fuel consumption and power output curves for the engine. For the 1300 RPM case, a fuel flow rate of 0.09726 g/cycle/cylinder or 6.322 g/s for the entire engine was predicted through the CFD computations.

For the 3300 RPM case, a fuel flow rate of 0.1305 g/cycle/cylinder or 21.532 g/s for the entire engine was predicted through the CFD computations.

The air inlet conditions were specified explicitly as initial conditions of the cylinder regime, since the air intake and exhaust process using moving valves was not modelled in this study. The initial conditions were determined taking into account the variable pre-compression and resulting temperature effects of the turbocharger and intercooler. Further, the initial swirl movement of the in-cylinder gases at BDC due to the air-intake process was approximated and modelled using Bessel functions.

TABLE II. INLET CONDITIONS

Rpm	1300	3300
P_{in}	187.5 kPa	385 kPa
T_{in}	357.6 K	384.66
Injection timing	-15° CA	-43.6°CA

The combustion model utilized in this study was a single step kinetic model describing the oxidation of the hydrocarbon fuels based on the well-defined DF2 fuel model as a presentative fuel for the Diesel fuel.

$$2\,C_{12}H_{26} + 37\,O_2 \rightarrow 24\,CO_2 + 26\,H_2O \quad (1)$$

Due to the relatively slow formation of thermal NOx, a 3-step kinetic mechanism representing the Extended Zeldovich Mechanism was utilized to accurately predict the formation of oxides of nitrogen. The following reactions were considered in this model:

$$O_2 + 2\,N_2 \rightarrow 2\,N + 2\,NO \quad (2)$$

$$2\,O_2 + N_2 \rightarrow 2\,O + 2\,NO \quad (3)$$

$$N_2 + OH \rightarrow 2\,H + 2\,NO \quad (4)$$

All other chemical reactions, including the hydrogen reactions, were modeled as chemical equilibrium reactions, as these reactions occur much faster than the relatively slow hydrocarbon oxidation thermal NOx reactions and can thus with reasonable accuracy be modeled as being at chemical equilibrium at each time step.

In the presented study, hydrogen was added on volume fraction basis. An initial hydrogen-oxygen mixture at stoichiometric ratio (2/3 H_2, 1/3 O_2 by mole fraction), as would be the result of a hydrolysis process was assumed. This H_2-O_2 mixture was then was premixed with the ambient air inlet gases, simulating ingestion of the H_2-O_2 mixture in the air inlet. The following nomenclature is used to refer to the different cases:

H0 – base case without hydrogen

H1 – 1%vol H_2-O_2 mixture

H3 – 3%vol H_2-O_2 mixture

III. RESULTS

A. *1300 rpm case*

The results of this study indicate significant effects through the addition of small amounts of H_2-O_2mixture into the inlet gases on the performance of the engine. **Error! Reference source not found.** and **Error! Reference source not found.** summarize the results of the 1300 RPM case. Brake mean effective pressure (bmep) increases with H_2-O_2 addition, resulting in increased power output. This leads to efficiency increases of 2.5% and 2.9% for 1% and 3% H_2-O_2 ingestion respectively with respect to the Diesel combustion, neglecting the additional chemical energy added through the hydrogen addition. However, when the heating value of hydrogen is taken into effect, thermal efficiency first increases by 1.3% for 1% H_2-O_2 ingestion but decreases by 0.5% with respect to the baseline as H_2-O_2 ingestion is increased to 3%.

Furthermore, **Error! Reference source not found.** shows that the exhaust pressure and temperature increase with H_2-O_2 fractions. As with power output, bmep and efficiency, the exhaust temperature and pressure show a significant increase with the ingestion of 1% H_2 and diminishing returns as H_2-O_2 ingestion is increased to 3%.

The thermal NOx emissions increase with H_2-O_2 fraction, due to facilitation of thermal NOx formation through higher combustion temperatures. Carbon dioxide emissions increase by 4.5% for the 1% hydrogen case, indicating more complete combustion of the hydrocarbon fuel but are reduced to 1.5% above the baseline value for the 3% hydrogen case, showing a reduction in hydrocarbon burn as compared to the previous case.

TABLE III. 1300 RPM, ENGINE PERFORMANCE

Case:	H0	H1	H3
bmep [KPa]	1336	1427	1441
Power [kW/cyl]	14	15	15.1
Power [kw]	84.1	89.9	90.8
Thermal Efficiency [%][a]	37.7	40.2	40.6
Thermal Efficiency [%][b]	37.7	39	37.2

a. Hydrogen is not included in efficiency calculations

b. Hydrogen is considered as fuel, H_2 heat release considered in thermal efficiency

TABLE IV. 1300 RPM, EXIT CONDITIONS PER POWER CYCLE AT 180 DEGREE CA ATDC

Case:	H0	H1	H3
Exit NO [g]	0.051	0.071	0.083
Exit CO [g]	0.017	0.028	0.031
Exit CO2 [g]	1.367	1.428	1.387
Pressure [KPa]	651	676	684
Average Temperature [K]	1187	1231	1254

Fig. 10 depicts the average in-cylinder temperature throughout the engine cycle. It can be observed that the average temperature rises more quickly with the addition of the H_2-O_2 mixture as soon as the injection event occurs at -15 degrees bTDC, as observed by the steeper temperature slopes. While the rate of temperature rise appears nearly identical for with hydrogen ingestion cases, the peak temperature rise is more significant in the H3 case than in the H1 case. The average temperature stays elevated throughout the engine cycle, as compared to the base case without hydrogen addition.

Fig. 11 shows the average in-cylinder pressure. Similar to the temperature, pressure rises more quickly with the onset of combustion and a significant increase in peak pressure is observed at 5 degrees aTDC, with peak pressure occurring at the same crank angle for all cases.

Fig. 12 depicts the concentration of gaseous fuel throughout the cylinder. The steeper slopes for the H1 and H3 case show that fuel evaporation rates are increased with hydrogen ingestion. This can be attributed to the fast initial burn of hydrogen and oxygen, facilitating fuel evaporation throughout the cylinder and later in the cylinder through increased combustion rates resulting in overall elevated temperatures and higher heat release rates, aiding evaporation after the initial hydrogen combustion and leading to an increased availability of gaseous fuel throughout the engine cycle.

Fig. 13 depicts the formation of oxides of nitrogen, which occurs mainly through the thermal NOx mechanism between TDC and 20 degrees aTDC, where temperatures are highest during the main combustion event and quickly normalizes as temperatures decrease during the expansion stroke. Through the early hydrogen combustion, a small increase in the nitrogen oxide formation prior to TDC is observed. With increased amounts of hydrogen addition, the rate of formation of NOx increases, as seen by the steeper slopes. This is due to the higher temperatures inside the cylinder, favoring NOx production, as well as the higher relative oxygen concentration. Overall, NOx emissions are increased significantly through the addition of hydrogen, increasing by as much as 50% in the case of 3% H_2-O_2 addition.

As shown in Fig. 14, the amount of water produced increases with H_2-O_2 addition, as expected, due to the recombination of the additional hydrogen and oxygen during the combustion process.

Fig. 15, shows that CO2 emissions increase notably with the ingestion of 1% H_2-O_2 mixture, but are reduced almost back to the baseline levels as H_2-O_2ingestion is increased further. This indicates that the degree of completion of hydrocarbon combustion first increased with hydrogen ingestion, then reaches a maximum and finally decreased as a critical percentage of H_2-O_2 is ingested.

The figures in appendix A and B depict iso-surface plots at 950K, 1800K and 2500K for temperature distributions and nitrogen oxide mass fractions of 0.004, 0.01 and 0.015 respectively.

Fig. 2 depicts the development of the fuel spray pattern and temperature distribution throughout the cylinder at -10°, 0° and 10° crank angle for the baseline case without hydrogen addition at 1300 rpm. The effect of the initial swirl is clearly observable, distorting and breaking up the fuel spray cones through the initial clockwise fluid motion of the in-cylinder gases. This helps break up the fuel and aids evaporation. At -10° CA, the spray cone is well defined and spray impingement on the piston bowl has not occurred. The combustion is initiated in the spray breakup zones at a slightly clockwise-displaced position from the spray cones as indicated by the small high temperature zones.

TDC marks the end of the injection event with fuel evaporating from the remaining spray cones as well as from the unburned fuel previously impinged on the from the hot piston bowl surface. The main combustion zones extend from the spray breakup zones clockwise of the spray cone to the piston bowl wall.

At 10° aTDC, the spray cones have completely dissipated and some remaining fuel is evaporating from the piston bowl walls. The combustion zone is thus attached to the piston bowl wall with somewhat lower temperatures present at the center of the bowl.

Fig. 3 shows similar fuel spray and temperature distributions for the 3% H_2-O_2 (H3) ingestions case. While the general trends remain the same, some distinct differences are observable. At -10° crank angle, the spray cones appear more spread out and less dense, indicating improved fuel evaporation. Further, the high temperature combustion zones clockwise of the spray cones in the H3 case appear significantly larger and further developed than in the base case, indicating earlier onset of ignition through the addition of hydrogen.

As the combustion propagates throughout the cylinder from TDC to 10° aTDC, the 3% hydrogen addition continues to show further development of the combustion as evidenced by the much larger high temperature zones. Again, re reduction in the liquid fuel particle density is observed, as the increased temperatures aid in fuel evaporation and combustion occurs more quickly to consume the vaporized fuel.

Fig. 4 and Fig. 5 compare the amount of NOx present in the cylinder for the base case and the 3% hydrogen ingestion case. At -10 degrees crank angle, no notable amounts of NOx are formed in either case, due to insufficient temperatures for this reaction to take place.

At top dead center, the hydrogen case produces NOx throughout high temperature combustions zones, while the NOx production of the base case is mostly contained to small regions at the center of each spray cone's combustion zone, further emphasizing the significant temperature differences between the two cases. After top dead center, the hydrogen case continues to produce more NOx. While both cases indicate NOx production effectively throughout the piston bowl, the iso-surfaces show that the amount of NOx produced in the hydrogen ingestion case is significantly higher and less confined to hotspots than in the base case.

B. 3300 rpm case

Error! Reference source not found. and **Error! Reference source not found.** summarize the results

of the 3300 RPM case. At an engine speed of 3300 rpm, ingestion of the hydrogen-oxygen mixture into the inlet gases produce power increases similar in magnitude as those observed in the 1300 rpm case. Unlike in the low engine speed case, diminishing returns with respect to power output with increased hydrogen ingestion from 1 to 3 % are, however, not observed but are proportionally related over the investigated range. This leads linear increase in Diesel-based thermal efficiency with increased hydrogen ingestion. However, taking into account the heating value of the ingested hydrogen, net thermal efficiency decreases with increasing hydrogen percentage. This can be attributed to significantly larger amount of H_2-O_2 mixture ingested at higher engine speeds and the associated energy required producing it.

Error! Reference source not found. shows that the exhaust pressure and temperature increase with ingested H_2-O_2 fractions, as would be expected due to the high combustion temperature of hydrogen. Decreasing carbon monoxide emissions and increasing carbon dioxide production are evidence of a more complete energy conversion of the fuel with increasing H_2-O_2 addition. The amount of oxides of nitrogen on the other hand increases with H_2-O_2 fraction, due to the higher combustion temperatures, allowing for more NOx to form.

TABLE V. 3300 RPM, ENGINE PERFORMANCE

Case:	H0	H1	H3
bmep [KPa]	1946	2014	2118
Power [kW/cyl]	51.9	53.2	56.4
Power [kW]	311.4	319.2	338.4
Thermal Efficiency [%][a]	32.7	33.6	35.6
Thermal Efficiency [%][b]	32.7	32.4	32.2

c. Hydrogen is not included in efficiency calculations

d. Hydrogen is considered as fuel and its heat release reduces the thermal efficiency

TABLE VI. 3300 RPM, EXIT CONDITIONS AT 180 DEGREE CA PER POWER CYCLE

Case:	H0	H1	H3
Exit NO [g]	0.003	0.009	0.009
Exit CO [g]	7.86E-06	6.96E-04	3.38E-04
Exit CO2 [g]	0.278	0.303	0.31
Pressure [KPa]	991.1	1009.8	1097.2
Average Temperature [K]	1051	1060	1150

Fig. 17 shows the average in-cylinder temperature throughout the engine cycle. Average temperature shows a rapid increase with the addition of the 3 percent H_2-O_2 mixture just after the fuel injection event. This signifies the high temperature combustion of the H_2-O_2 mixture just before TDC and before the main fuel combustion and results in an increased peak temperature. The rapid increase in temperature is much more prominent in the 3300 rpm case than in the low engine speed case. At 1% H_2-O_2 mixture, the peak temperature is still elevated compared to the baseline case, however, the sharp initial rise in temperature is not observed. The average temperature then stays elevated throughout the engine cycle, as compared to the base case without hydrogen addition.

Fig. 18 shows the average in-cylinder pressure. Analogous to the temperature curve, pressure increases much more rapidly for the 3% H_2-O_2 case. Overall, pressure increases with hydrogen addition.

Fig. 19 shows the development of oxides of nitrogen throughout the engine cycle. Addition of H_2-O_2 clearly increases the amount of NO formation as a result of higher temperatures. It should be noted that although the average temperatures for base case and 1 percent H_2-O_2 addition are comparable at the end of the cycle, the majority of the thermal NOx formation occurs right after TDC at peak temperatures, where temperatures are high enough to accelerate the reaction.

As shown in Fig. 20, the amount of water produced increases with H_2-O_2 addition, as expected, due to the recombination of the additional hydrogen and oxygen during the combustion process and show initial spikes due to the fast hydrogen combustion prior to the Diesel combustion event.

Fig. 21 shows that CO2 emissions increase with the addition of hydrogen and oxygen, indicating a more complete burn, especially in regards to converting the remaining fuel at the end of the combustion process due to higher temperatures in the expansion stroke, leaving less unburned hydrocarbons.

Fig. 6 and Fig. 7 depict the spray patterns and temperature distribution and Fig. 8 and Fig. 9 show the NOx distributions throughout the cylinder. These show significant differences to the low engine speed case. At 1300 rpm, the combustion event was initiated in the outer regions of the fuel spray cones. At higher engine speeds, ignition occurs at cylinder bowl wall and propagates inward. This trend is emphasized by the ingestion of hydrogen, resulting in larger and hotter primary ignition zones at -10° CA.

At TDC, the fuel spray is less dense and more scattered in the case of hydrogen ingestion. In this case, the high temperature combustion zones are more prominent at the cylinder wall and lower temperatures are encountered at the center of the bowl, as compared to the baseline case without hydrogen ingestion. At 10° aTDC, the density of liquid fuel particles is much higher in the case with hydrogen ingestion, suggesting a overall slower burn that lasts longer into the expansion stroke.

Thermal NOx is produced as early as -10° CA near the primary ignition zone at the cylinder wall, as

opposed to the low engine speed case, which did not show NOx production at this point. The majority of the thermal NOx from TDC on is produced near the cylinder wall, which is the location of the hottest burn within the cylinder.

IV. CONCLUSION:

It was shown that for both 1300 and 3300 RPM cases, the ingestion of a stoichiometric hydrogen-oxygen mixture into the inlet gases, significant benefits with respect to power production can be achieved for the Yanmar 6LY2A-STP Turbo-Diesel marine engine. Diminishing returns were observed at 1300 rpm when hydrogen fraction was increased from 1% to 3 % but were not observed at the increased engine speed of 3300 rpm. These benefits in power production are a result of increased in-cylinder pressures and temperatures due to increased heat release rates. The hydrogen causes a slight advancement in ignition, improved evaporation of the Diesel fuel and more complete energy conversion of the Diesel fuel. Increased completion of the fuel burn along with the combustion of hydrogen and oxygen resulted in increased CO2 and H2O emissions and higher combustion temperatures resulted in increased thermal NOx production in all cases.

Overall, net thermal efficiency was decreased in nearly all cases due to the energy required to produce the hydrogen. However, the case of 1300 rpm and 1% H_2-O_2 mixture resulted in an increase in net efficiency of 1.3%. This leads to the conclusion that on-board hydrogen production is not feasible in most cases through utilization of the output power through e.g. alternators, but may be a viable approach if energy recuperation systems such as exhaust thermal energy extractors are used to produce the hydrogen.

It is suggested, that the benefits of hydrogen injection may be increased through adjustment of the injection timing, in order to offset the effects of ignition advancement through hydrogen injection. Further, a more in-depth investigation of the chemical-kinetic interactions occurring during the combustion of a hydrocarbon/hydrogen fuel mixture may further help improve the utilization potential of hydrogen ingestion.

REFERENCES

[1] M. P. Poonia, A. Ramesh and R. Gaur, "Experimental investigation of the factors affecting the performance of a LPG - Diesel dual fuel engine," SAE International, 1999.

[2] S. Quadri, . M. Masood and P.R. Kumar, "Effect of pilot fuel injection operating pressure in hydrogen blended compression ignition engine: An experimental analysis," Fuel, vol. 157, p. 279–284, 2015.

[3] F.W. Hoehn, "advances in ultralean combustion technology using hydrogren-enriched gasoline," IEEE Transactions on Aerospace and Electronic Systems 11 (5), pp. 958-958, 1975.

[4] G. Fontana, "Performance and fuel consumption estimation of a hydrogen enriched gasoline engine at part-load operation," SAE Technical Paper Series, Vols. 2002-01-2196, p. 4–5, January, 2002.

[5] D. L. Mathur H.B., "Performance characteristics of a hydrogen fueled SI engine using timed manifold injection," Int. J. Hydrogen Energy, vol. 16, pp. 115-117, 1991.

[6] Per Tunestal, "hydrogen addition for improved lean burn capability of slow and fast natural gas combustion chambers," SAE Technical Paper Series, Vols. 2002-01-2686, January, 2002.

[7] Boonthum Wongchai, "Cylinder pressure variations of the fumigated hydrogen-Diesel dual fuel combustion," American Journal of Applied Sciences, vol. 9, no. 12, pp. 1967-1973, 2012.

[8] G. N. N. Saravanan, "experimental investigation in optimizing the hydrogen fuel on a hydrogen Diesel dual-fuel engine," Energy & Fuels, vol. 23, p. 2646–2657, 2009.

[9] F. Christodoulou, Hydrogen, Nitrogen and Syngas Enriched Diesel, Brunel University, 2014.

[10] W. B. Santosoa, "Combustion characteristics of Diesel-hydrogen dual fuel engine at low load," Energy Procedia, no. 32, pp. 3-10, 2013.

[11] H. Zhang, "effects of hydrogen addition on nox emissions in hydrogen-assisted Diesel combustion," in International Multidimensional Engine Modeling Users Group Meeting Detroit, Detroit, 2009.

[12] Wall J, Effect of hydrogen enriched hydrocarbon combustion on emissions and performance. Panacea University (2008).

[13] M. Deb, "Hydrogen-Diesel combustion on a single cylinder Diesel engine," Journal of Applied Sciences Research, vol. 8, no. 9, pp. 4806-4814, 2012.

[14] Prateep Chaisermtawan, "Gaseous emissions and combustion efficiency analysis of hydrogen-Diesel dual fuel engine Under Fuel-Lean Condition," American Journal of Applied Sciences, vol. 9, no. 11, pp. 1813-1817, 2012.

A. A. Buzukov, "Ignition and combustion of a hydrogen-air mixture," Combustion, Explosion, and Shock Waves, vol. Vol. 35, no. No. 6, pp. 601-611, 1999.

V. APPENDIX

A. In-cylinder visualization for 1300 rpm case

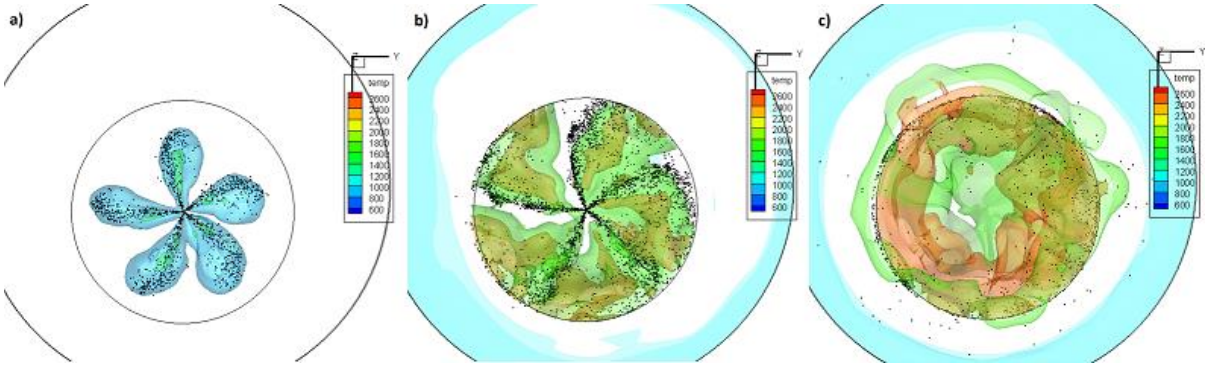

Fig. 2. Case H0 Temperature Profiles at 1300 RPM at a) -10 deg b) 0 deg and c) +10 deg aTDC

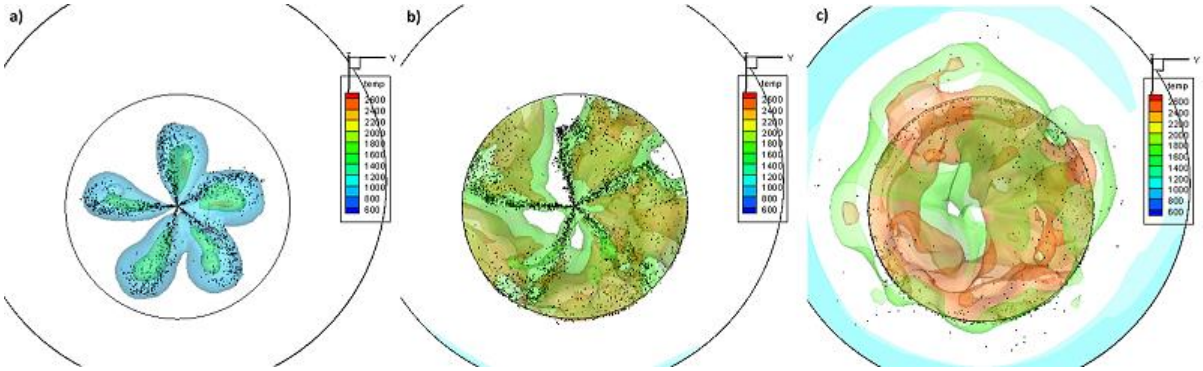

Fig. 3. Case H3 Temperature Profiles at 1300 RPM at a) -10 deg b) 0 deg and c) +10 deg aTDC

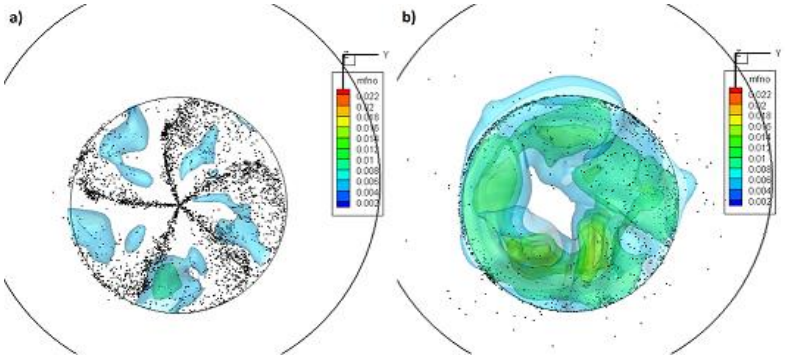

Fig. 4. Case H0 NOx Distribution Profiles at 1300 RPM at a) 0 deg and b) +10 deg aTDC

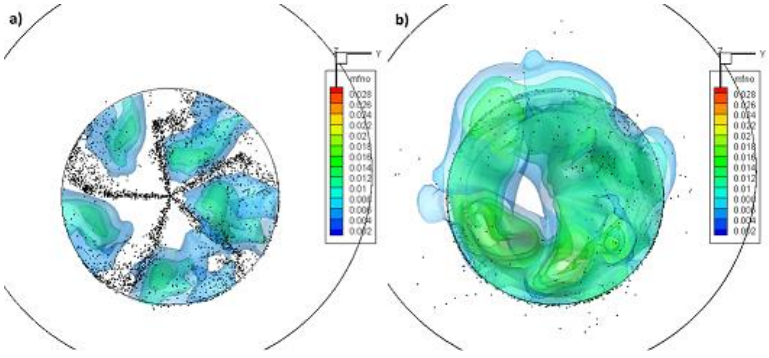

Fig. 5. Case H3 NOx Distribution Profiles at 1300 RPM at a) 0 deg and b) +10 deg aTDC

B. In-cylinder visualization for 3300 rpm case

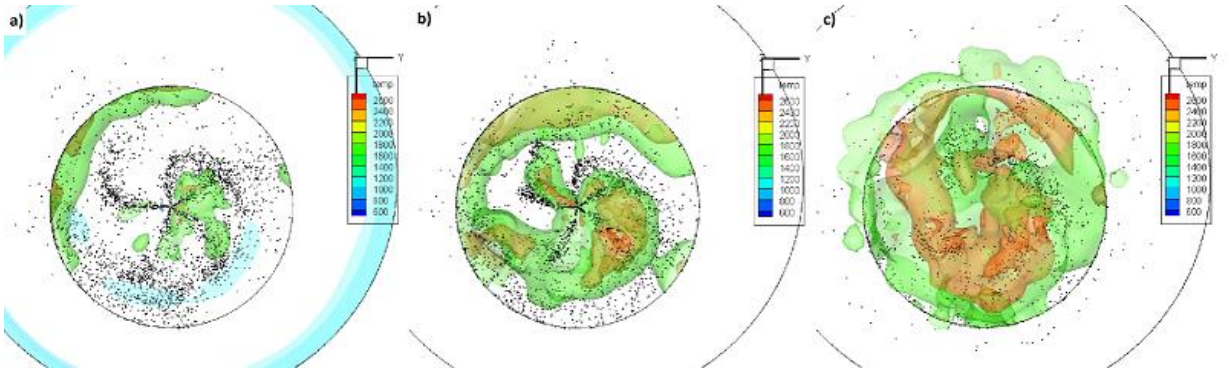

Fig. 6. Case H0 Temperature Profiles at 3300 RPM at a) -10 deg b) 0 deg and c) +10 deg aTDC

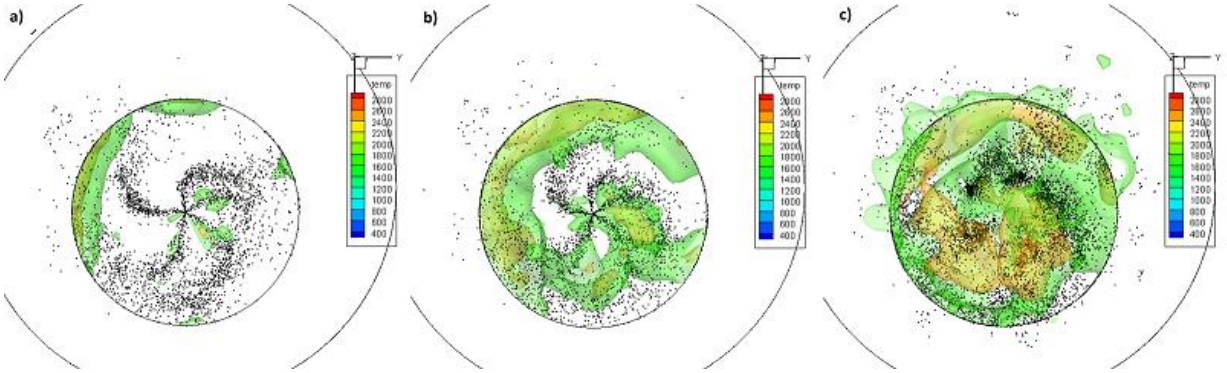

Fig. 7. Case H3 Temperature Profiles at 3300 RPM at a) -10 deg b) 0 deg and c) +10 deg aTDC

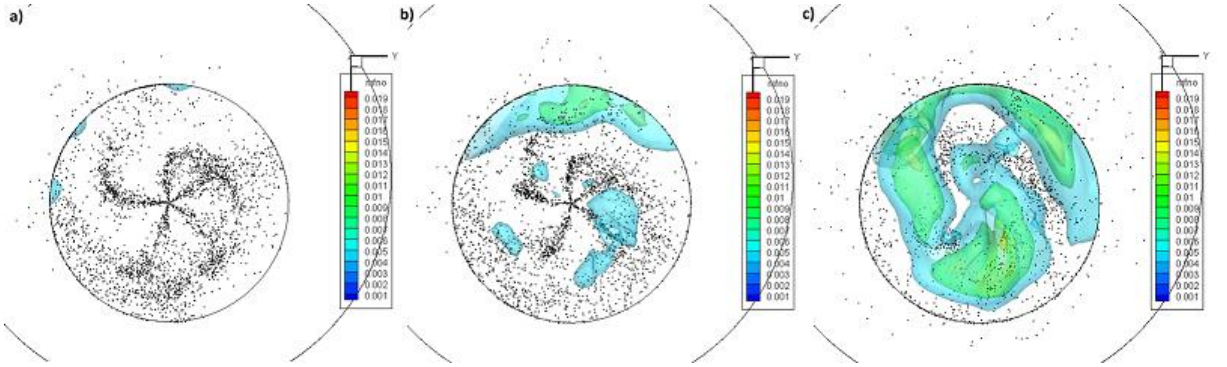

Fig. 8. Case H0 NOx Distribution Profiles at 3300 RPM at a) -10 deg b) 0 deg and c) +10 deg aTDC

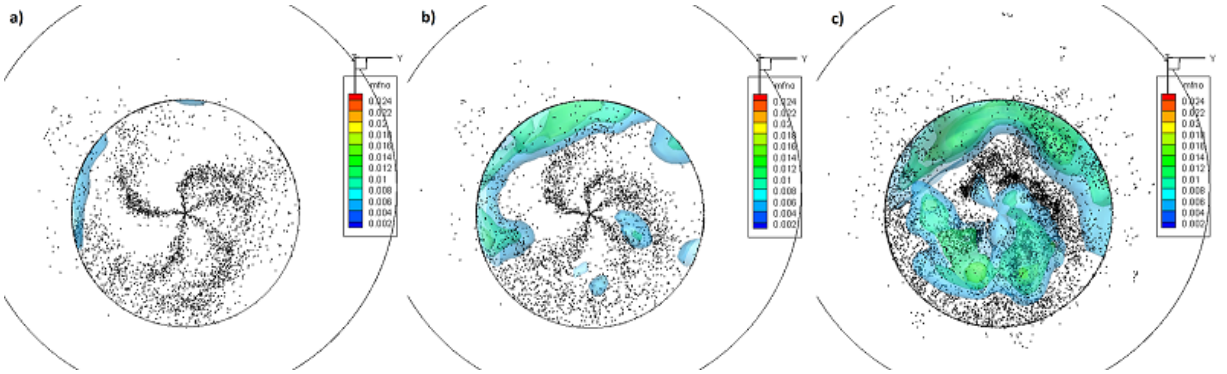

Fig. 9. Case H3 NOx Distribution Profiles at 3300 RPM at a) 0 deg b) +5 deg and c) +10 deg aTDC

C. *Cycle Analysis Figures for 1300 RPM case*

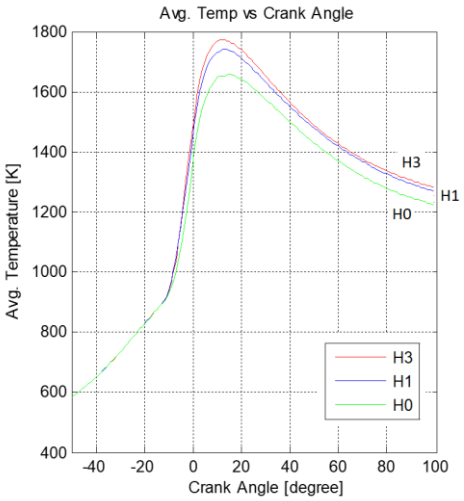

Fig. 10. 1300 RPM, Average Temperature vs CA

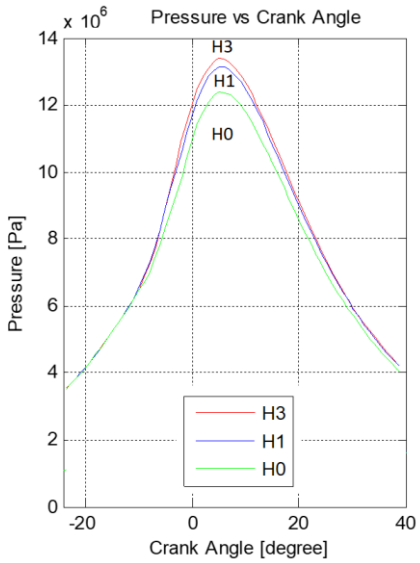

Fig. 11. 1300 RPM, Pressure vs CA

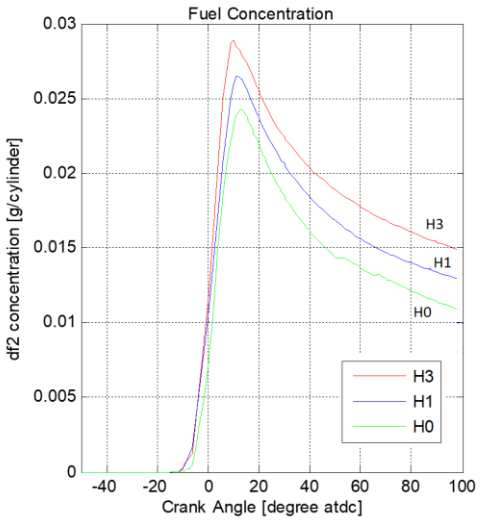

Fig. 12. 1300 RPM, Gaseous Fuel Concentration vs CA

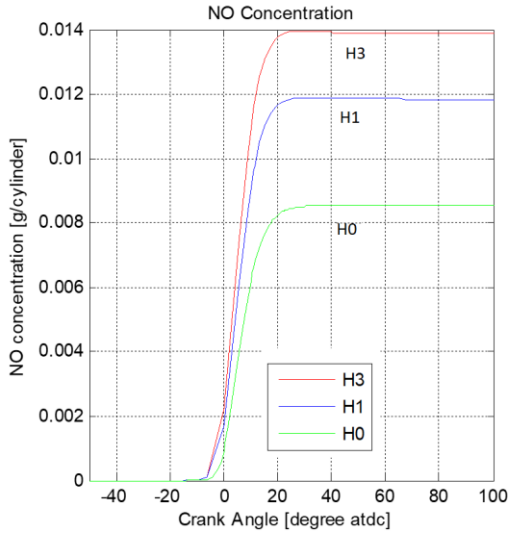

Fig. 13. 1300 RPM, NOx vs CA

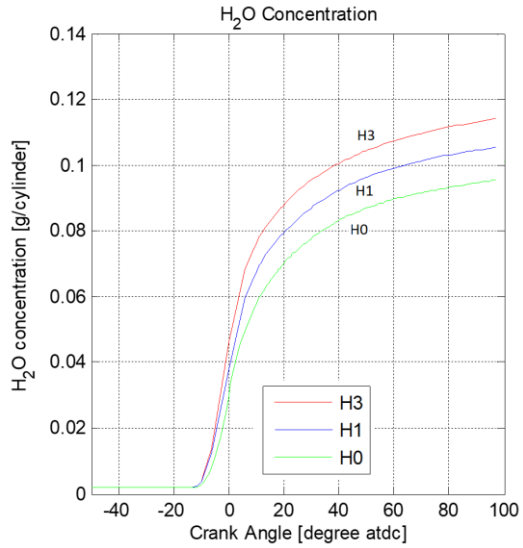

Fig. 14. 1300 RPM, H2O vs CA

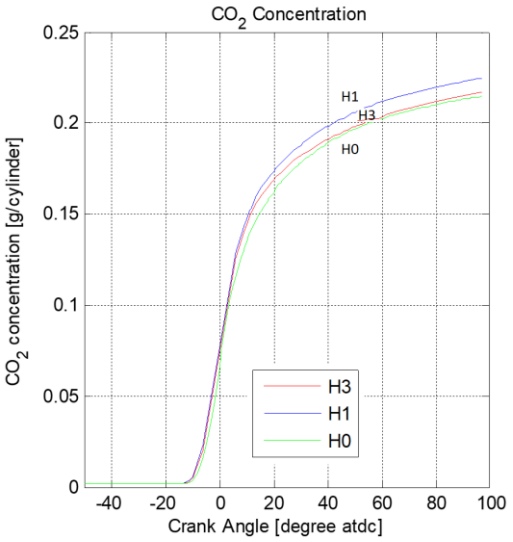

Fig. 15. 1300 RPM, CO2 vs CA

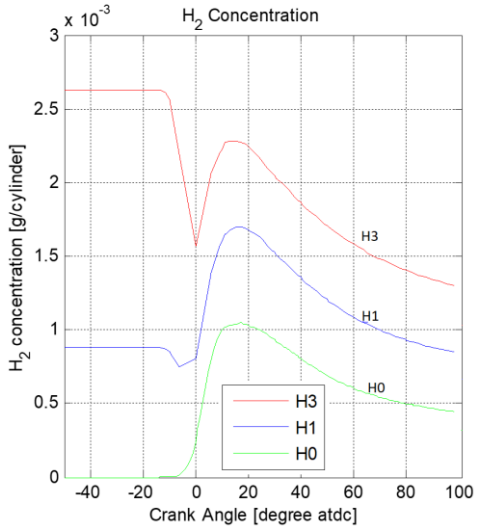

Fig. 16. 1300 RPM, H2 vs CA

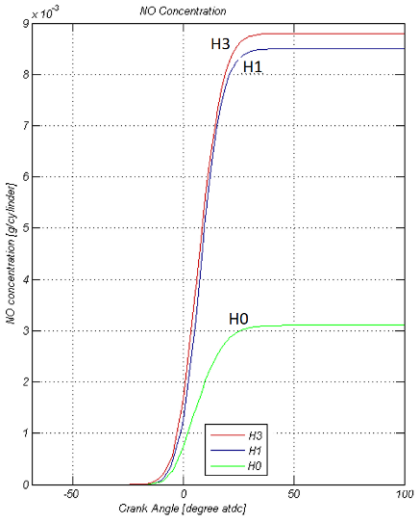

Fig. 19. 3300 RPM, NOx vs CA

D. Cycle Analysis Figures for 3300 RPM case

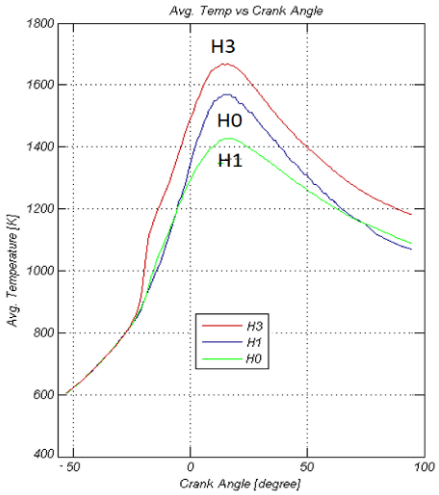

Fig. 17. 3300 RPM, Average Temperature vs CA

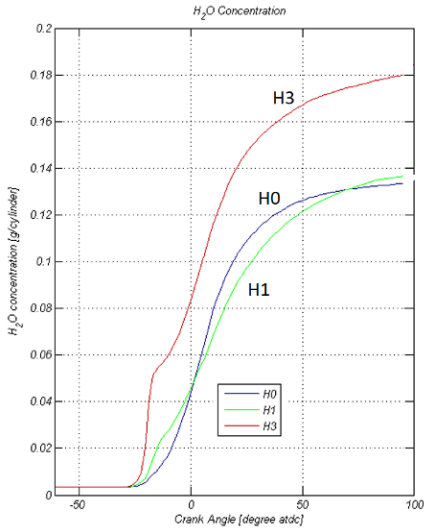

Fig. 20. 3300 RPM, H2O vs CA

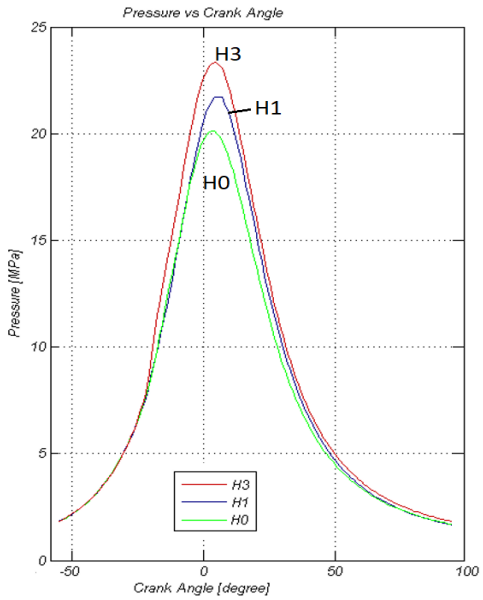

Fig. 18. 3300 RPM, Pressure vs CA

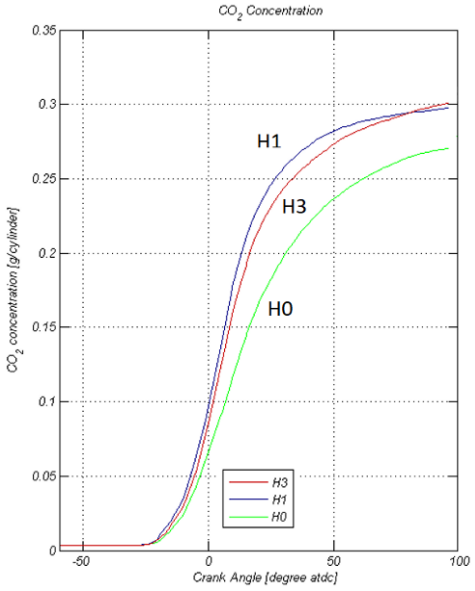

Fig. 21. 3300 RPM, CO2 vs CA